TECTONICS, VOL. 18, NO. 4, PAGES 621-638, AUGUST 1999

Thermochronologic constraints on deformation and cooling history of high- and ultrahigh-pressure rocks in the Qinling–Dabie orogen, eastern China

Laura E. Webb,[1,2] Bradley R. Hacker,[3] Lothar Ratschbacher,[4] Michael O. McWilliams,[1] and Shuwen Dong[5]

Abstract. The Hong'an block is the best place to study the exhumation of high-pressure (HP) and ultrahigh-pressure (UHP) metamorphic rocks in the Qinling–Dabie orogen of eastern China because it lacks the extensive Cretaceous tectonic and thermal overprint observed in the Dabie Shan. We measured timing of deformation and rate of cooling of the HP–UHP rocks by $^{40}Ar/^{39}Ar$ analyses of synkinematic minerals from tectonites of key structural zones in the Hong'an and Tongbai Shan. Normal-sense shear along the north dipping Huwan detachment at the northern edge of the Hong'an block occurred between 237 and 231 Ma; this detachment facilitated the bulk of the exhumation of the HP–UHP rocks. Our new $^{40}Ar/^{39}Ar$ ages, combined with U/Pb zircon and Sm/Nd ages of 245–240 Ma, suggest that exhumation of UHP rocks from mantle depths occurred at rates of 5–25 mm/yr from ~245 to 230 Ma. The mountain range is a warped extensional footwall, within which white mica cooled from 225 to 205 Ma. Locally, younger extension is recorded by white mica recrystallization at 198–194 Ma, after which the entire block had cooled to below 300 °C. Early Cretaceous $^{40}Ar/^{39}Ar$ ages from the Tongbai shear zone indicate that dextral shear along the southwest boundary of the orogen was contemporaneous with normal to sinistral-oblique slip along the Xiaotian–Mozitan fault along the northern boundary. Coeval dextral and sinistral shear zones along the northern and southwestern margins of the Hong'an and Dabie Shan would have caused eastward lateral extrusion of these two blocks, perhaps driven by collision of the Lhasa block with Eurasia.

1. Introduction

Ultrahigh-pressure (UHP) rocks of the Qinling–Dabie orogen, eastern China, attest to the subduction of crustal rocks to depths > 100 km during the Triassic collision between the Yangtze and Sino–Korean cratons. Study of this UHP orogen enhances our understanding of the dynamics of collision zones, the link between physical processes operating at deep and shallow structural levels within orogenic belts during exhumation and the Mesozoic tectonic evolution of Asia. The Hong'an block, the westward continuation of the Dabie Shan, provides the best opportunity to study the exhumation of high-pressure (HP)–UHP metamorphic rocks in the orogen because it lacks the extensive Cretaceous tectonic and thermal overprint observed in the Dabie Shan [*Hacker et al.*, 1995; *Webb et al.*, 1996]. The Hong'an block also contains a pseudostratigraphy that reveals the geometry of tectonic denudation structures at the orogen scale. We report new $^{40}Ar/^{39}Ar$ ages from fault and shear zones and cross cutting plutons that constrain the timing of Mesozoic tectonism in the orogen and cooling rates of once deeply subducted continental crust.

1.1. Regional Geology

The west-northwest trending Qinling–Dabie orogen marks the boundary between the Sino–Korean and Yangtze cratons (Figure 1). Subduction along the southern margin of the Sino–Korean craton occurred during both the middle Paleozoic and early Mesozoic. The Qinling–Dabie orogen is characterized by juxtaposition of the ~400 Ma North Qinling–Tongbai metamorphic belt and the ~220 Ma South Qinling–Dabie metamorphic belt [*Mattauer et al.*, 1985] (Figure 2). Both are cut by active, east trending, sinistral strike-slip faults related to the India–Asia collision [*Peltzer et al.*, 1985].

The South Qinling–Dabie complex formed during Triassic collision between the Yangtze and Sino–Korean cratons. Paleomagnetic data suggest that the Yangtze and Sino–Korean cratons did not fully converge until at least Late Triassic time [*Lin et al.*, 1985; *Opdyke et al.*, 1986] and that the Yangtze craton was oriented ~60° counter clockwise from its present orientation prior to the Middle Triassic. These data suggest that the collision progressed from east to west, closing an intervening oceanic basin as the Yangtze craton rotated with respect to the Sino–Korean craton [e.g., *Enkin et al.*, 1992].

During collision, ultrahigh-pressure and high-pressure metamorphic rocks formed in a north dipping subduction zone. These rocks are exposed in the easternmost Tongbai, Hong'an, Dabie, and Su–Lu ranges. Voluminous Triassic flysch deposits in the Songpan-Ganze region of west central China represent detritus produced by erosion of the South Qinling–Dabie complex [*Yin and Nie*, 1993; *Zhou and Graham*, 1996; *Brugier et al.*, 1997] (Figure 1). A magmatic arc associated with subduction during the Mesozoic has yet to be discovered, although a few Triassic granitoids crop out in the

[1]Department of Geological and Environmental Sciences, Stanford University, Stanford, California.

[2]Now at Section des Sciences de la Terre, University of Geneva, Geneva, Switzerland

[3]Department of Geological Sciences, University of California at Santa Barbara.

[4]Institute for Geology, University of Wuerzburg, Wuerzburg, Germany.

[5]Institute of Geomechanics, Chinese Academy of Geological Sciences, Beijing.

Paper number 1999TC900012.
0278-7407/99/1999TC900012$12.00

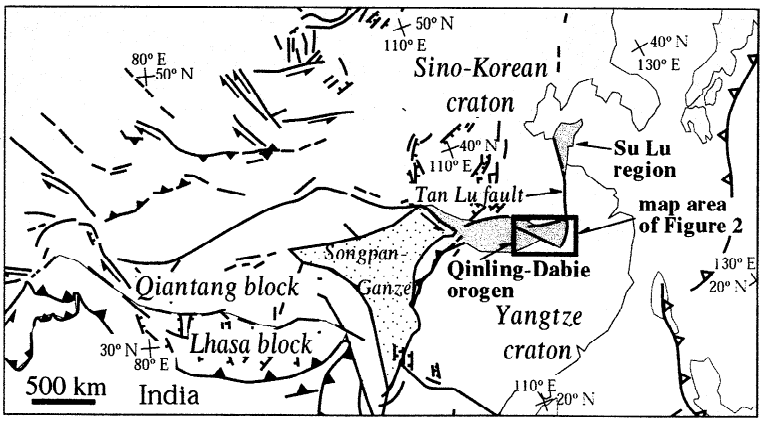

Figure 1. Regional geologic map of central Asia (modified after *Peltzer and Tapponnier* [1988]) illustrating locations of the Qinling–Dabie orogen and tectonic elements discussed in text. Rectangle depicts map area shown in Figure 2.

Qinling region. The main body of the arc may have been displaced laterally by strike-slip faulting [*Mattauer et al.*, 1985] or completely eroded during exhumation of the HP–UHP rocks.

HP–UHP metamorphic rocks form the core of the Qinling–Dabie orogen in the Dabie Shan and Hong'an regions. North dipping detachment faults define the northern topographic limit of both regions and separate high-grade rocks from greenschist-facies rocks of the Foziling Group [cf. *Hacker et al.*, 1996b] (Figure 2). Regionally, the HP–UHP units trend subparallel to the NW trend of the orogen. Inferred metamorphic pressures and temperatures increase northward across the orogen. Peak pressures > 3 GPa are recorded by eclogite bodies found as blocks or boudins within phengite and/or biotite quartzofeldspathic schists and gneisses [*Zhang et al.*, 1993], which locally also contain the UHP indicator minerals coesite and diamond [*Wang and Liou*, 1991]. These features suggest that the HP–UHP units were subducted and exhumed as a coherent slab. Each unit has undergone retrograde greenschist- and amphibolite-facies metamorphism, and all are intruded by Cretaceous plutons [*Hacker et al.*, 1995].

The Tan Lu fault marks the eastern boundary of the Dabie Shan (Figure 2). Approximately 500 km of sinistral strike-slip motion during the Triassic–Jurassic has been postulated on the basis of apparent offset of the Dabie and Su–Lu UHP terranes [*Okay and Sengör*, 1992; *Yin and Nie*, 1993] (Figure 1). The tectonic significance and age of the fault are still a matter of debate. No apparent Triassic–Jurassic structures associated with the Tan Lu have been identified in the Dabie Shan. However, the Cenozoic Tan Lu is morphologically well expressed, dips steeply east, and has normal to dextral-oblique displacement recorded by cataclasites and slickensides with lower greenschist-facies minerals [*Hacker et al.*, 1995]. Cretaceous extension by normal and sinistral strike-slip faulting throughout the orogen may be kinematically related to Pacific margin transtension [*Hacker et al.*, 1995] and indentation tectonics of south central Asia (L. Ratschbacher et al., manuscript in preparation, 1999). Cretaceous northwest–southeast extension is most pronounced in the Dabie Shan, where synkinematic plutons of intermediate compositions form the northern half of the range [*Hacker et al.*, 1998].

1.2. Previously Published Age Data

The Triassic collision between the Yangtze and Sino–Korean cratons is documented by a growing body of post collisional cooling ages in the range of 245–170 Ma [*Chen et al.*, 1992; *Li et al.*, 1989a, b, 1993; *Okay et al.*, 1993; *Eide et al.*, 1994; *Hacker and Wang*, 1995; *Ames et al.*, 1996; *Rowley et al.*, 1997; *Xue et al.*, 1997; *Hacker et al.*, 1998]. *Ames et al.* [1996] and *Rowley et al.* [1997] reported U/Pb zircon ages of ~220 Ma from UHP eclogites and host gneisses and interpreted these to be the age of peak UHP metamorphism. More recently, *Hacker et al.* [1998] found a second population of ~240 Ma metamorphic overgrowths on single zircon grains from the UHP unit in the Dabie Shan with sensitive high-resolution ion microprobe (SHRIMP) techniques. The Early Triassic zircon ages agree with Sm/Nd ages of ~245 Ma reported by *Li et al.* [1993] and *Okay et al.* [1993]. The $^{40}Ar/^{39}Ar$ cooling ages from Dabie Shan micas typically range from 218 to 180 Ma for the HP–UHP metamorphic rocks [*Hacker and Wang*, 1995]. The spatial distribution of the Dabie Shan ages is complex, but in the Hong'an block, *Eide et al.* [1994] reported an apparent south-to-north decrease in phengite ages from schists and gneisses. These ages range from 225 Ma in the blueschist unit to 195 Ma in the eclogite units. The older-to-younger trend parallels the northward increase in metamorphic grade.

U/Pb ages for zircons from igneous and metamorphic rocks in the northern orthogneiss unit of the Dabie Shan range from 137 to 128 Ma [*Hacker et al.*, 1998; *Xue et al.*, 1997]. The $^{40}Ar/^{39}Ar$ ages obtained from mica and hornblende from these same rocks range from 133 to 122 Ma [*Hacker and Wang*, 1995]. Similar ages for plutons in the Hong'an and Tongbai Shan were obtained by *Li and Wang* [1991], *Eide* [1993], and *Ames et al.*, [1996] and range from 132 to 119 Ma.

2. Structural Setting of Hong'an and Eastern Tongbai Shan Samples

The especially clear pre-Cretaceous structure of the Hong'an block, with respect to the overprinted Dabie Shan, forms the framework for understanding the radiometric ages.

Figure 2. Simplified geologic map of the Qinling–Dabie orogen comprising the Tongbai Shan, Hong'an, and Dabie Shan regions. Letters used for ages of sedimentary units are the following: S, Sinian; P, Permian; T, Triassic; J, Jurassic; K, Cretaceous; and E, Eocene. (Map compilation is based our observations, *RGS Anhui* [1987], *RGS Henan* [1989], and *RGS Hubei* [1990]).

In the Hong'an block, penetrative south dipping foliation, south plunging stretching lineation, lineation-parallel isoclinal folds, and regionally consistent kinematic indicators in the eclogite and amphibolite units reflect high-strain deformation and top-to-north coaxial flow of the HP–UHP rocks (Figures 3 and 4) (Webb, L.E et al., Mesozoic tectonics in the Hong'an and Tongbai Shan of the Qinling–Dabie collisional orogen, China: Implications for the exhumation of ultrahigh-pressure rocks, submitted to *Special Paper of the Geological Society of America*, 1999 (hereinafter referred to as Webb et al., submitted manuscript, 1999); B. R. Hacker et al., manuscript in preparation, 1999). Foliations and lineations in eclogite blocks typically parallel those of host schists and gneisses. Along the northern margin there is an important transition to north dipping foliation and top-to-north shear sense, indicating that the Hong'an block is a warped extensional footwall. Deformation

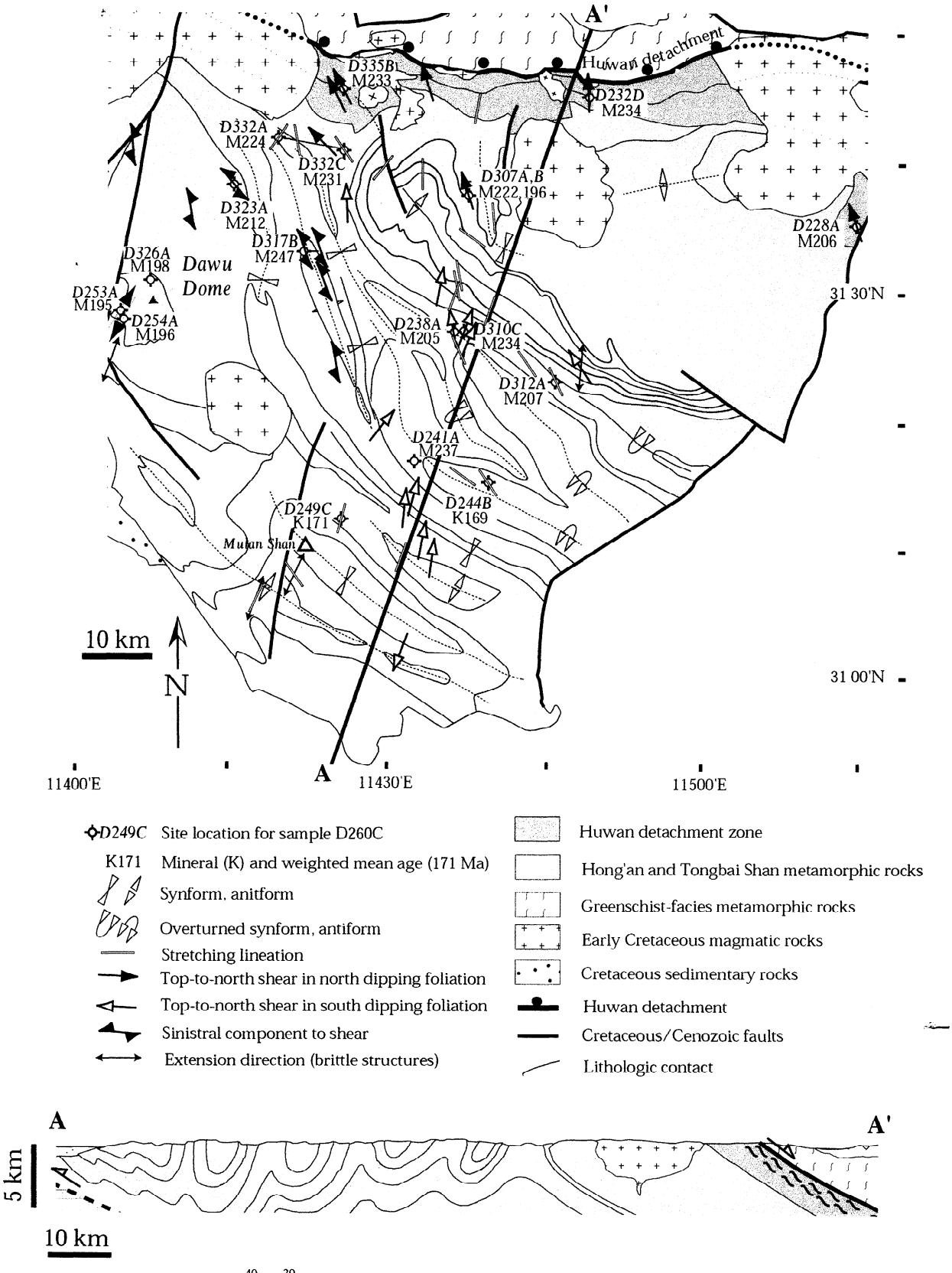

Figure 3. Locations of $^{40}Ar/^{39}Ar$ samples and kinematic map for Triassic–Jurassic ages and structures in the Hong'an block and schematic cross section illustrating rollover of foliation (~200% vertical exaggeration). Ages reported are weighted mean ages in mega annum. M, white mica; B, biotite; K, K-feldspar. (Map is based on our observations, *RGS Henan* [1989] and *RGS Hubei* [1990]).

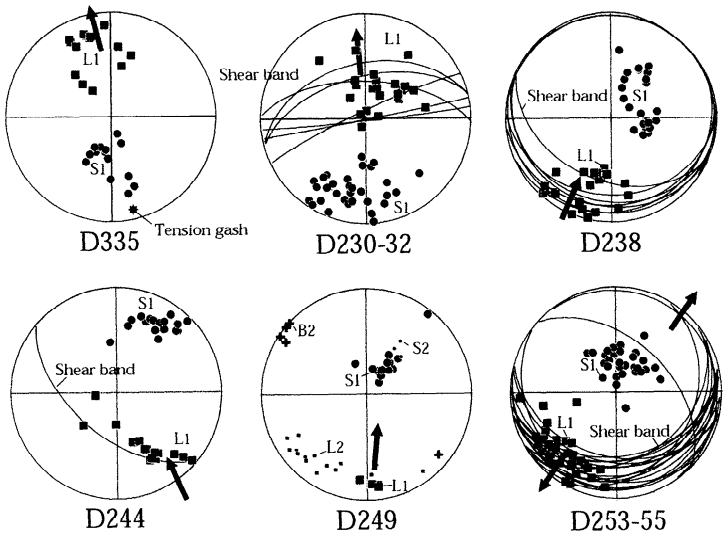

Figure 4. Representative structural data for $^{40}Ar/^{39}Ar$ samples that gave Triassic–Jurassic ages. Data are depicted in equal-area, lower hemisphere projection stereonets. Localities are shown in Figure 3. Lettered annotations of data are the following: S, pole to foliation; L, stretching lineation; B, fold axes. Number refers to generation of structure.

was accompanied by decompression and syntectonic recrystallization at eclogite- and amphibolite-facies conditions from upper mantle through midcrustal depths [*Rowley and Xue*, 1996; *Webb et al.*, 1996]

A second stage of coaxial deformation is observed throughout the block and is best viewed in ductile to ductile-brittle structures at Dawu Dome (Figure 3). The dome is characterized by a felsic gneissic core mantled by blueschist- to greenschist-facies metasedimentary rocks. These rocks are cut by north and south dipping shear bands with normal-sense displacement. Fault slip data from older ductile-brittle to brittle faults at Dawu and elsewhere in the Hong'an region, together with late stage tension gashes (Webb et al., submitted manuscript, 1999), indicate similar northeast–southwest subhorizontal extension during the latest stages of cooling and decompression.

In the Tongbai Shan a major northwest trending amphibolite-facies dextral shear zone involves both metasedimentary and igneous rocks of the Tongbai Complex and appears to continue west to the Nanyang basin (our observations and *Regional Geological Survey Henan* [1989]) (Figure 5). A northwest trending, sinistral strike-slip fault overprints the southern margin of the Tongbai dextral shear zone and deforms Early Cretaceous plutons and red beds under greenschist- to subgreenschist-facies conditions. This fault may be related to strike-slip faults that form the southern boundary between blueschist-facies rocks and the fold-and-thrust belt south of the Dabie Shan [*Hacker et al.*, 1995].

3. New $^{40}Ar/^{39}Ar$ Data From Hong'an and Eastern Tongbai Shan Regions

We measured the timing of deformation and rate of cooling of the Hong'an and Tongbai Shan HP–UHP rocks by $^{40}Ar/^{39}Ar$ analyses of synkinematic minerals from tectonites of the Huwan detachment, Dawu Dome, and Tongbai shear zone. We also dated two cross cutting plutonic bodies from the northern Hong'an and Tongbai Shan, providing an upper limit on the timing of deformation of the Huwan detachment. Samples included white mica, biotite, potassium feldspar separates, and one pseudotachylite whole rock (Table 1). White mica, ubiquitous in the host paragneisses and common in mylonitized eclogites, was assumed to be either muscovitic or phengitic based on paragenesis. The $^{40}Ar/^{39}Ar$ analyses were conducted at the Stanford University geochronology laboratory (see *Hacker et al.* [1996a] for analytical details). Typically, all samples gave highly radiogenic gas fractions requiring atmospheric corrections of 10% or less, and less than 5% on average for white mica, in particular.

3.1. Synkinematic Minerals From Triassic–Jurassic Structures

The oldest group of white mica ages from the Hong'an block include those obtained from mylonitized eclogites and quartzofeldspathic schists and gneisses associated with top-to-north normal shear sense along the Huwan detachment (Figures 3 and 6). D232D, a mylonitic quartzofeldspathic schist, gave a spectrum that is internally discordant over the bulk of the ^{39}Ar released and yields a weighted mean age (WMA) of 235 ± 2 Ma. This age is within error of the total fusion age (TFA) and inverse isochron age (IIA). The isochron for the chosen steps, although poorly fit, shows that the released gas was a binary mix of radiogenic and atmospheric ^{40}Ar.

White mica samples from another Huwan detachment locality gave conflicting ages. D335A was separated from a mylonitized eclogite in which kinematic indicators (e.g., garnet σ and δ clasts) indicate top-to-north shear. In thin section the white mica is synkinematic, defining the lineation and growing in porphyroclast pressure shadows. The apparent age spectrum has a concave-upward shape with maximum appar-

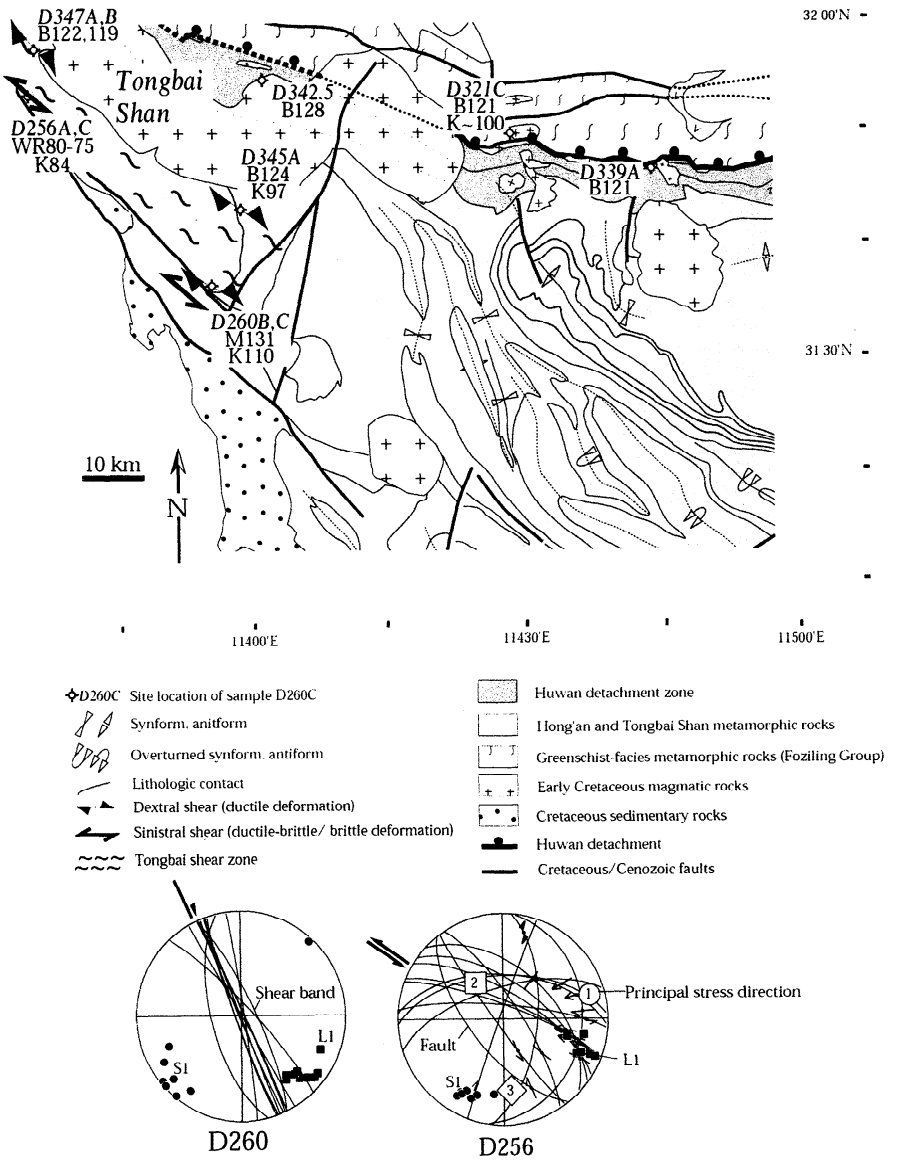

Figure 5. Locations of $^{40}Ar/^{39}Ar$ samples and kinematic map for Cretaceous ages and structures in the eastern Tongbai Shan. Ages reported are weighted mean ages in mega annum. M, white mica; B, biotite; K, K-feldspar; WR, pseudotachylite. Representative structural data for samples that gave Cretaceous $^{40}Ar/^{39}Ar$ ages are depicted in equal-area, lower hemisphere projection stereonets. Lettered annotations of data are the following: S, pole to foliation; L, stretching lineation; B, fold axes. (Map is based on our obsevations, *RGS Henan* [1989] and *RGS Hubei* [1990]).

ent ages of ~350 Ma at the low- and high-temperature ends. This sample yielded a TFA of 319 ± 3 Ma and a WMA of 310 ± 3 Ma for the intermediate steps. Because the spectrum has the saddle shape often characteristic of excess ^{40}Ar and the ages are older than reported U/Pb zircon ages [*Ames et al.*, 1996; *Rowley et al.*, 1997; *Hacker et al.*, 1998], we consider this age suspect and probably geologically meaningless.

A white mica separate (D335B) from a top-to-north shear band within the quartzofeldspathic gneiss that hosts the previous sample (D335A) gave an age more consistent with the 235 Ma WMA obtained from D232D. Although the spectrum is internally discordant, the TFA and WMA agree within error, at 232 ± 2 and 235 ± 2 Ma.

Similar Middle Triassic white mica cooling ages were also obtained from two samples from the hanging wall of the detachment. D310C, a mylonitized eclogite showing top-to-north shear, gave 234 ± 1 Ma for both the WMA and IIA. A mica schist, D241A, yielded a WMA of 237 ± 2 Ma, consistent with both the TFA and IIA. The saddle-shaped spectrum and $^{40}Ar/^{36}Ar$ intercept of 2419 ± 1342 possibly indicate excess ^{40}Ar. However, we choose not to dismiss the age data due to the large $^{40}Ar/^{36}Ar$ intercept error and the fact that the obtained TFA, WMA, and IIA ages are consistent with one another, as well as with those from D232D, D335B, and D310C, all localities exhibiting top-to-north shear.

White mica samples D332A and D332C come from the

Table 1. Summary of $^{40}Ar/^{39}Ar$ data

Sample Number	Latitude North, deg	Longitude East, deg	Mineral Dated	TFA, Ma	WMA, Ma	IIA, Ma	$^{40}Ar/^{36}Ar$ Intercept	MSWD
D228A	31°30.5'	115°17.7'	WM	205 ± 2	206 ± 2	206 ± 2	294 ± 6	0.3
D232D	31°45.5'	114°53.0'	WM	235 ± 2	234 ± 2	234 ± 2	309 ± 35	17
D238A	31°26.8'	114°38.8'	WM	201 ± 2*	203 ± 2*	203 ± 2	842 ± 129	0.5
D241A	31°13.3'	114°34.8'	WM	236 ± 2	237 ± 2	235 ± 2	2419 ± 1344	3.1
D244B	31°14.1'	114°38.5'	KFS	163 ± 2	169 ± 2	163 ± 3	338 ± 19	5.7
D249C	31°09.4'	114°27.5'	KFS	158 ± 2	171 ± 2	170 ± 3	319 ± 82	37
D253A	31°28.7'	114°06.6'	WM	195 ± 2*	194 ± 2*	194 ± 2	499 ± 48	2.5
D254A	31°28.4'	114°06.9'	WM	196 ± 2	196 ± 2	197 ± 2	258 ± 23	0.5
D256A	31°56.6'	113°38.6'	KFS	83.9 ± 0.8	83.4± 0.8	80.5 ± 2.5	430 ± 102	6.8
D256C	31°56.6'	113°38.6'	WR	75.4 ± 0.7	74.9 ± 0.8	74.9 ± 0.8	590 ± 111	0.6
D260B	31°37.1'	113°58.2'	WM	130 ± 1	131 ± 1	132 ± 1	224 ± 19	4.6
D260C	31°37.1'	113°58.2'	KFS	120 ± 1	110 ± 1	103 ± 1	649 ± 15	2.1
D307A	31°36.5'	114°41.9'	WM	218 ± 2	222 ± 2	221 ± 2	365 ± 43	1.0
D307B	31°36.5'	114°41.9'	WM	195 ± 2	196 ± 2	195 ± 2	543 ± 262	26
D310C	31°26.6'	114°39.6'	WM	233 ± 1	234 ± 1	234 ± 1	299 ± 13	2.6
D312A	31°20.8'	114°47.9'	WM	208 ± 1	207 ± 1	206 ± 1	383 ± 17	0.8
D317B	31°32.4'	114°26.8'	WM	243 ± 2	247 ± 2	243 ± 6	528 ± 460	29
D321C	31°50.0'	114°32.1'	BIO	121 ± 1	121 ± 1	121 ± 2	300 ± 110	9.6
D321C	31°50.0'	114°32.1'	KFS	98 ± 1	101 ± 1	87 ± 8	846 ± 641	1.6
D323A	31°37.7'	114°18.9'	WM	213 ± 2	212 ± 1	211 ± 2	506 ± 220	20
D326A	31°31.4'	114°09.9'	WM	198 ± 2	198 ± 2	198 ± 2	344 ± 73	12
D332A	31°42.1'	114°23.2'	WM	222 ± 2	224 ± 2	225 ± 2	143 ± 61	4.4
D332C	31°42.0'	114°26.1'	WM	232 ± 2	231 ± 2	229 ± 3	405 ± 110	11
D335A	31°45.3'	114°28.4'	WM	319 ± 3	310 ± 3	313 ± 4	153 ± 53	106
D335B	31°45.3'	114°28.4'	WM	232 ± 2	233 ± 2	211 ± 11	4471 ± 4691	10
D339A	31°44.6'	114°43.4'	BIO	119 ± 1	121 ± 1	120 ± 2	580 ± 307	3.8
D342.5	31°56.0'	114°04.9'	BIO	118 ± 1	130 ± 1	128 ± 2	552 ± 95	1.5
D345A	31°44.3'	114°02.1'	BIO	123 ± 1	124 ± 1	124 ± 1	367 ± 61	2.0
D345A	31°44.3'	114°02.1'	KFS	105 ± 2	97 ± 3	96 ± 4	318 ± 71	0.5
D347A	32°00.6'	113°43.7'	BIO	120 ± 1	122 ± 1	121 ± 1	423 ± 74	1.0
D347B	32°00.6'	113°43.7'	BIO	119 ±1	119 ±1	119 ±1	289 ±8	0.2

WM, white mica; KFS, potassium feldspar; WR, pseudotachylite; BIO, biotite; IIA, inverse isochron age; WMA, weighted mean age; TFA, total fusion age; MSWD, mean square weighted deviation. The MSWD expresses goodness of fit index for inverse isochron. The $^{40}Ar/^{36}Ar$ intercept is the inherited argon component (295.5 is the atmospheric $^{40}Ar/^{36}Ar$ ratio).

*Indicates age obtained after spectrum was recalculated to account for excess ^{40}Ar (see text).

western end of the UHP unit. D332A, from a top-to-north shear band, yielded a WMA of 224 ± 2 Ma (Table 1 and Figure 7). D332C is from a mica-rich layer surrounding retrogressed eclogite and gave a WMA of 231 ± 2 Ma. Although both samples yield internally discordant step ages, the TFA, WMA, and IIA agree within error. White mica from a retrograde epidote-actinolite schist farther SE in the HP eclogite unit, D323A, gave a WMA of 212 ± 2 Ma.

Two white mica samples are from an eclogite locality in the UHP unit in north central Hong'an. Samples D307A and D307B came from mylonitized eclogite and host paragneiss, respectively, showing top-to-north normal to dextral-oblique shear. Although D307A did not yield a plateau and there is some disruption in the spectrum at the low-temperature end, we take the WMA of 222 ± 2 Ma to be a good estimate of the cooling age. The inverse isochron indicates that the gas was most likely a binary mixture of radiogenic and atmospheric argon. The WMA agrees with both the TFA and IIA. D307B gave a significantly younger age. The spectrum is internally discordant, with oldest ages at the low- and high-temperature ends of the spectrum. The saddle shape is suspicious, but the inverse isochron $^{40}Ar/^{36}Ar$ intercept of 543 ± 262, while poorly constrained, is not significantly different from that of atmosphere. Additionally, isotopic ratios do not indicate any Cl-correlated excess ^{40}Ar component. We interpret 195 ± 2 Ma (TFA and IIA) as a credible cooling age.

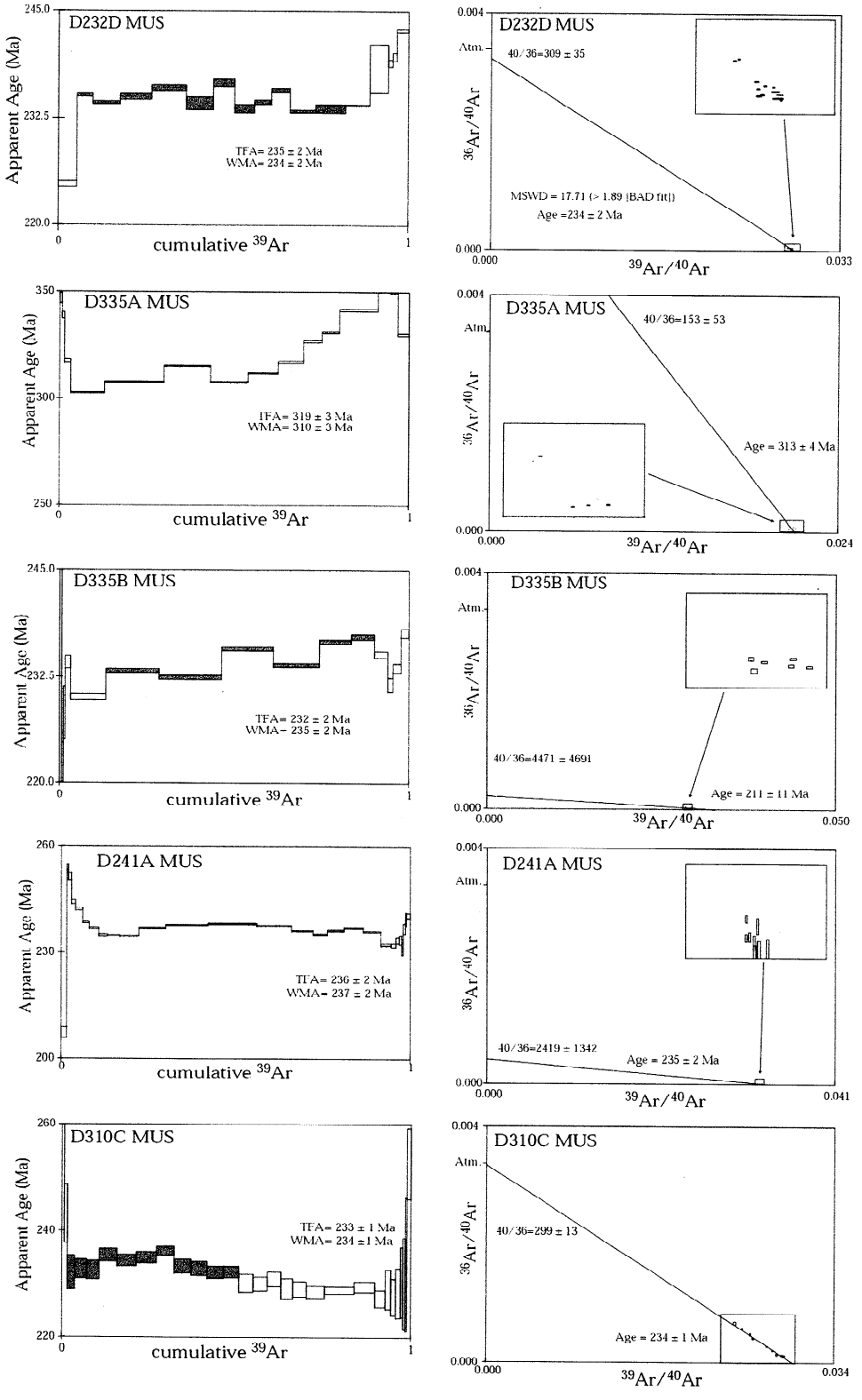

Figure 6. The ^{40}Ar/^{39}Ar age spectra and isotope correlation diagrams for white mica samples that gave Triassic–Jurassic ages (D232D, D335A, D335B, D241A and D310C). Weighted mean ages were calculated using solid steps. TFA, total fusion age; WMA, weighted mean age.

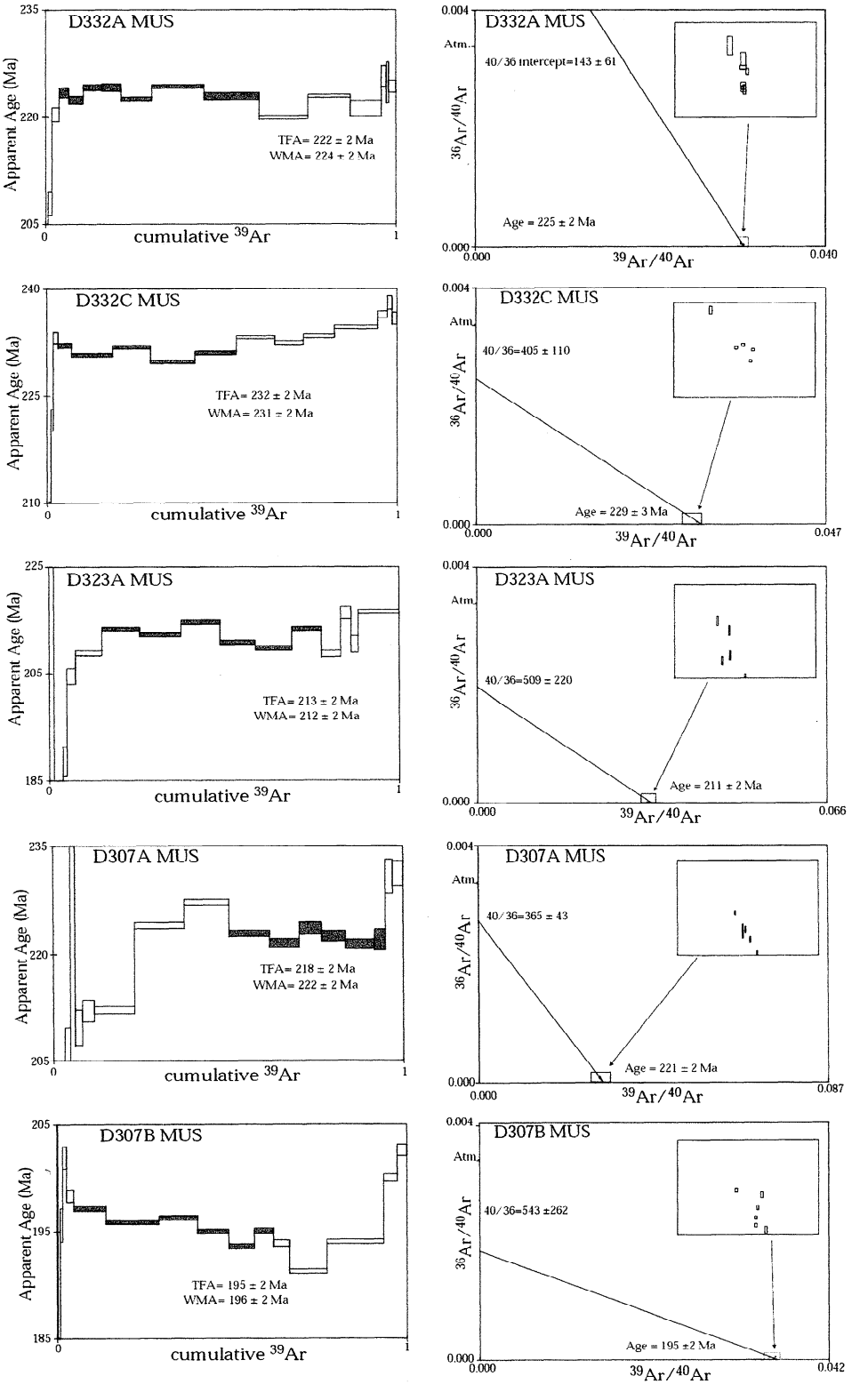

Figure 7. The ^{40}Ar/^{39}Ar age spectra and isotope correlation diagrams for white mica samples that gave Triassic–Jurassic ages (D332A, D332C, D323A, D307A, and D307B). Weighted mean ages were calculated using solid steps.

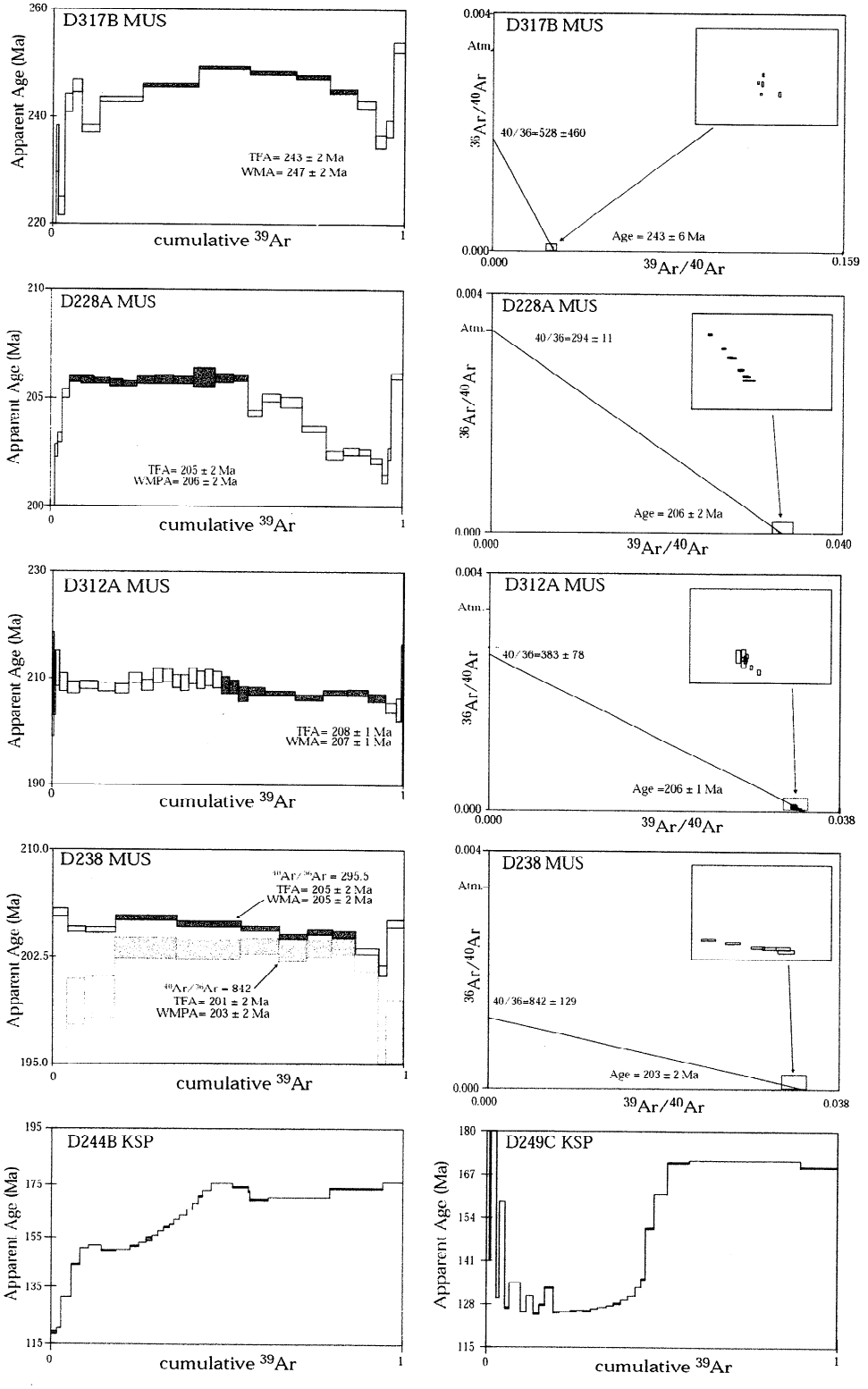

Figure 8. The ^{40}Ar/^{39}Ar age spectra and isotope correlation diagrams for samples that gave Triassic–Jurassic ages. Weighted mean ages were calculated using solid steps (D317B, D228A, D312A, D238, D244B, and D249C). Where two spectra are shown for a single sample, the older spectrum was calculated assuming a trapped ^{40}Ar/^{36}Ar ratio of 295.5, while the younger spectrum was calculated using the indicated ^{40}Ar/^{36}Ar ratio. WMPA, weighted mean plateau age.

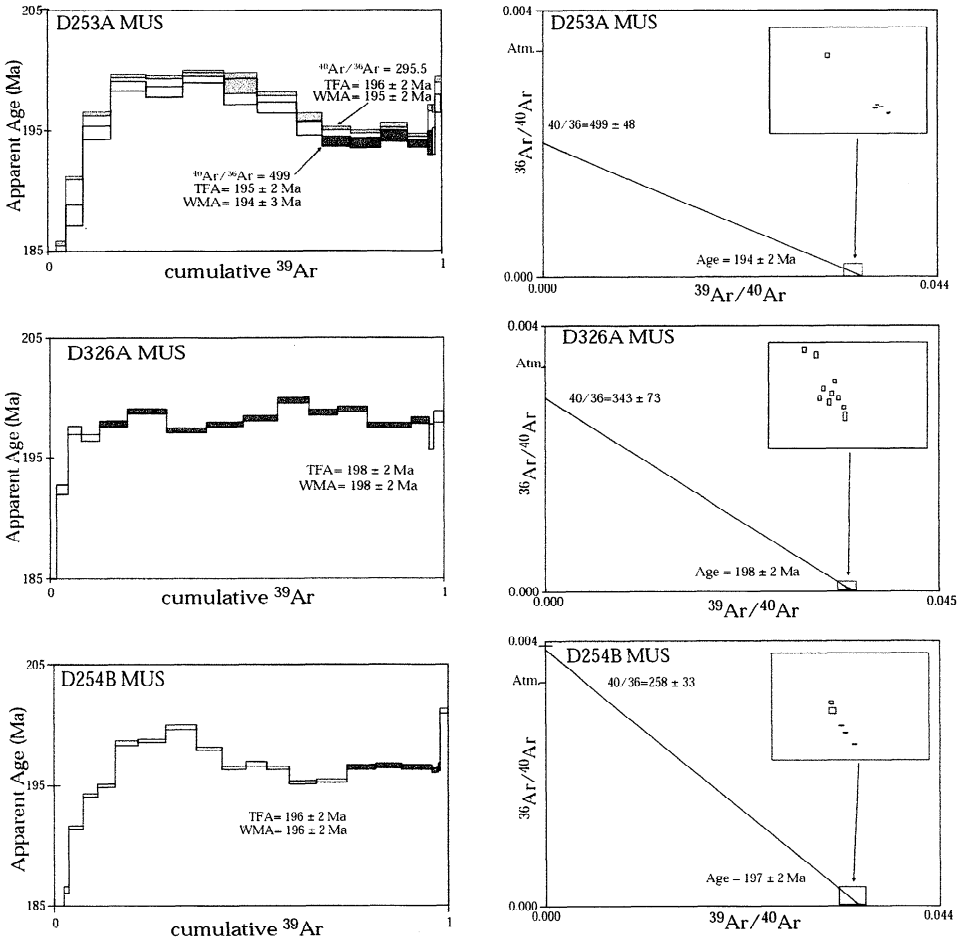

Figure 9. The ^{40}Ar/^{39}Ar age spectra and isotope correlation diagrams for white mica samples that gave Early Jurassic ages (D253A, D326A, and D254B). Weighted mean ages were calculated using solid steps. Where two spectra are shown for a single sample, the older spectrum was calculated assuming a trapped ^{40}Ar/^{36}Ar ratio of 295.5, while the younger spectrum was calculated using the indicated ^{40}Ar/^{36}Ar ratio.

D317B, a white mica separate from a top-to-north shear band cutting banded eclogite in the HP eclogite unit, gave a WMA of 247 ± 2 Ma (Figure 8). The hump shape of the apparent age spectrum suggests this is a maximum age for the sample. *Eide et al.* [1994] reported a TFA of 230 Ma from a phengitic gneiss at the same locality.

Paragneiss in the UHP unit in the northeast corner of the Hong'an block (D228A) gave a spectrum internally concordant for 50% of the total ^{39}Ar released and a weighted mean plateau age (WMPA) of 206 ± 2 Ma. Isochrons show that this subset of the data is linearly correlated and that the released gas was a binary mix of radiogenic and atmospheric argon. A similar WMA of 207 ± 1 Ma was obtained from a quartzofeldspathic gneiss, sample D312A, southeast of this last locality.

D238 is from a quartzofeldspathic gneiss in the HP eclogite unit. The isochron shows a strong negative linear correlation with a ^{40}Ar/^{39}Ar intercept of 842 ± 129. Figure 6 shows an age spectrum that is internally concordant for 68% of the ^{39}Ar released and yields a WMPA of 203 ± 2 Ma after recalculated to account for the excess ^{40}Ar.

Two feldspars from schists (D244B and D249C) in the HP units show complex spectra characterized by increasing step ages. The highest temperature steps of the experiments yielded ages in the range of 160–170 Ma for both samples. Younger ages at the low-temperature end of the spectra may represent Late Jurassic and Early Cretaceous cooling.

Three samples of synkinematic white mica from the quartzofeldspathic, gneissic core (D253A and D326A) and the overlying metasedimentary, schistose rocks (D254B) of Dawu Dome constrain the second stage of coaxial deformation. For D253A the isochron data are well correlated with an ^{40}Ar/^{36}Ar intercept of 499 ± 48 and a WMA of 195 ± 2 Ma (Figure 9). The age of D253A is given more credence by comparable ages from both D326A and D254B. For D254B a subset of the data in the inverse isochron shows a well-fit, negative linear correlation, and the ^{40}Ar/^{36}Ar intercept is not significantly different from that atmosphere. Like D253A, the spectrum is internally discordant and characterized by a hump shape in the first 60% of ^{39}Ar released. The high-temperature steps are more consistent and give a TFA of 196 ± 2 Ma, essentially equal to the IIA and weighted mean age (WMA).

D326A yielded a flatter, though still internally discordant, spectrum. Younger apparent ages in the low-temperature steps might be the result of argon loss. The TFA, WMA, and IIA all give an age of 198 ± 2 Ma.

3.2. Synkinematic Minerals From Cretaceous Structures and Minerals From Plutons and Thermal Overprint

We dated samples of synkinematic muscovite and biotite (D260B, D345A, D347A, and D347B) and K-feldspar (D260C) from the Tongbai dextral shear zone (Figure 5). White mica from D260B gave a spectrum with a slight hump shape. The bulk of the spectrum is relatively flat and gives a TFA of 130 ± 1 Ma and a WMA of 131 ± 1 Ma, both within error of the IIA (Figure 10). The inverse isochron indicates a trapped $^{40}Ar/^{36}Ar$ component of 224 ± 19, considerably lower than the atmospheric value. This value and the convex-down shape may indicate argon loss, though probably not significant. An Early Cretaceous age for deformation is further supported by the D260C K-feldspar spectrum. The oldest ages for the high-temperature steps range from 134 to 124 Ma, compatible with D260B.

Synkinematic biotite from two other localities in the Tongbai shear zone also support Early Cretaceous deformation. Sample D345A is a quartzofeldspathic gneiss in which mesoscopic kinematic indicators show dextral shear (Webb et al., submitted manuscript, 1999). More than 50% of the released ^{39}Ar yields concordant TFA, WMA, and IIA ages. We interpret the WMA of 124 ± 1 Ma to represent the cooling age of the biotite following deformation. We obtained a WMA of 97 ± 3 Ma from potassium feldspar from D345A, similar to the IIA of 96 ± 4 Ma. Similarly, D347A, a shear band cutting orthogneiss, gave a WMA of 122 ± 1 Ma. IIA $^{40}Ar/^{36}Ar$ intercepts for data subsets for both samples yielded results not significantly different from atmosphere. An orthogneiss sample from this locality (D347B) yielded a WMPA of 119 ± 1 Ma.

Two biotite samples were dated from different plutonic bodies in the northern Hong'an Block. D321C came from a granite stock north of the Huwan detachment. The spectrum, though not internally concordant, is fairly consistent and yields a WMA of 121 ± 1 Ma, compatible with its TFA and IIA (Figure 11). Potassium feldspar from sample D321 gave serially increasing ages. The data do not define a plateau, but we interpret the WMA of 101 ± 1 Ma as the cooling age. D342.5 is from the large pluton that intrudes the Huwan detachment. The WMA of 130 ± 1 Ma agrees well with the IIA and with 138–125 Ma K/Ar ages obtained from this pluton by Li and Wang [1991].

Sample D339A is from an orthogneiss that occurs as large xenoliths in hypabyssal granitic rocks intruded into the Huwan detachment zone. The biotite we dated is a static overgrowth on garnet in the gneiss. The TFA, WMA, and IIA all indicate cooling at 121 ± 1 Ma.

NW trending, sinistral strike-slip faults overprint the southern margin of the Tongbai dextral shear zone and deform Early Cretaceous plutons and red beds at greenschist- to subgreenschist-facies conditions. We determined the age of this deformation by dating a pseudotachylite (D256C) cutting mylonitic granite (D256A) in the Tongbai Shan. The spectrum shows serially increasing ages. A flatter portion of the pseudotachylite spectrum gives a WMA of 74.9 ± 0.8 Ma, consistent with the IIA. We believe this age to be the age of brittle faulting, as Late Cretaceous cooling is also inferred from the lower temperature steps of the K-feldspar $^{40}Ar/^{39}Ar$ spectrum from the same region (D256A).

4. Discussion

4.1. Triassic–Jurassic Ages and Tectonic Interpretations

We recognize three geologically meaningful groups of Triassic–Jurassic white mica ages (Figure 12): (1) ~237–230 Ma, reflecting deformation and cooling associated with extension along the Huwan detachment; (2) ~225–205 Ma, associated with recrystallization of phengite to muscovite following retrograde metamorphism at midcrustal levels; and (3) ~200–195 Ma, reflecting a second stage of extension and doming, as seen at Dawu.

4.1.1. Huwan detachment. Samples from two localities in the Huwan detachment zone gave WMA of 234 and 233 Ma, and cooling ages as old as 237 Ma were obtained from the UHP unit in the footwall of the detachment. These are among the oldest $^{40}Ar/^{39}Ar$ ages reported from the orogen. Similarly old ages from the Dabie Shan obtained by *Hacker and Wang* [1995] were considered dubious at that time because they predated the 220 Ma zircon ages of *Ames et al.* [1996]. Two lines of evidence now lend credence to phengite ages older than 220 Ma: (1) in Hong'an these phengites are now tied to a specific structural zone, the Huwan detachment, and (2) SHRIMP data from zircons from Dabie Shan and Hong'an indicate two Triassic stages of metamorphic growth of zircon: an older generation at ~240 Ma and a younger generation at ~220 Ma [*Hacker et al.*, 1998].

4.1.2. Retrograde metamorphism. The 240 Ma recrystallization of zircon (as well as Sm/Nd ages referenced in section 1.2) is interpreted to reflect peak pressure conditions, whereas the 220 Ma event may have been caused by thermal or fluid influx at crustal levels after the bulk of exhumation was complete [*Hacker et al.*, 1998]. We interpret the >225 Ma phengite ages as cooling during exhumation from mantle to crustal depths, facilitated, at least in part, by tectonic denudation following UHP metamorphism at ~240 Ma. Muscovite ages of 225–205 Ma are then related to retrograde metamorphism and recrystallization during exhumation through the crust.

4.1.3. Early Jurassic extension. Ages from synkinematic white mica in both the gneissic core and overlying metasedimentary rocks from Dawu Dome indicate that the 198–194 Ma population represents the age of northeast–southwest extension. The subhorizontal extension direction in the ductile fabrics is identical to the extension direction during ductile-brittle to brittle faulting at Dawu and elsewhere within the Hong'an block (Webb et al., submitted manuscript, 1999). Therefore, exhumation of the UHP rocks through upper crustal levels occurred by the Middle Jurassic in the Hong'an block. It is likely that the suite of 200–180 Ma ages of white mica in the Dabie Shan reported by *Hacker and Wang* [1995] reflects cooling during this same tectonic episode.

4.2. Implications for Exhumation Models and Rates

The data presented here and by others [e.g., *Eide*, 1993; *Rowley and Xue*, 1996; *Hacker et al.*, 1998] suggest that the

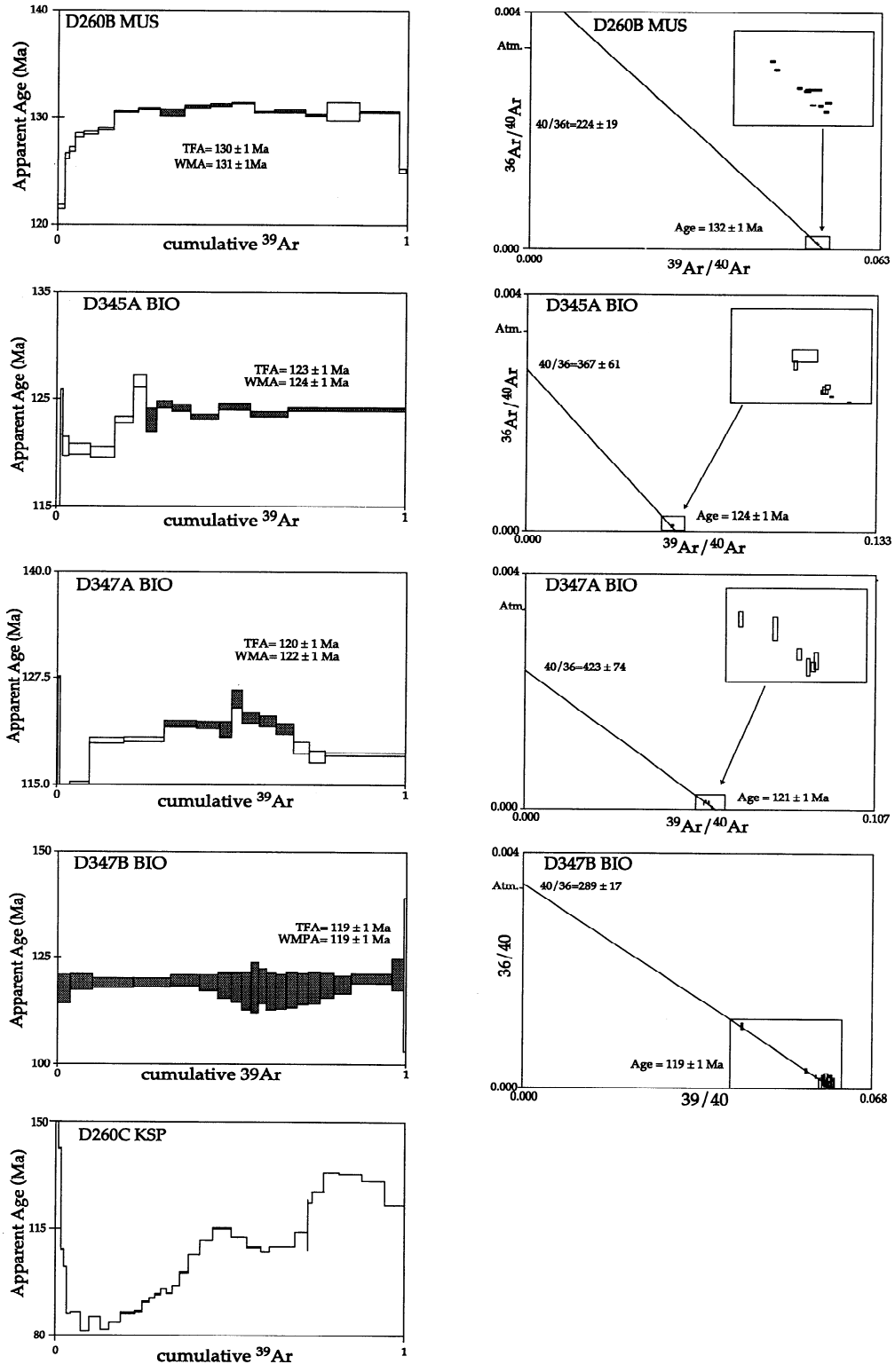

Figure 10. The ^{40}Ar/^{39}Ar age spectra and isotope correlation diagrams for samples that gave Cretaceous ages (D260B, D345A, D347A, D347B, and D260C). Weighted mean ages were calculated using solid steps.

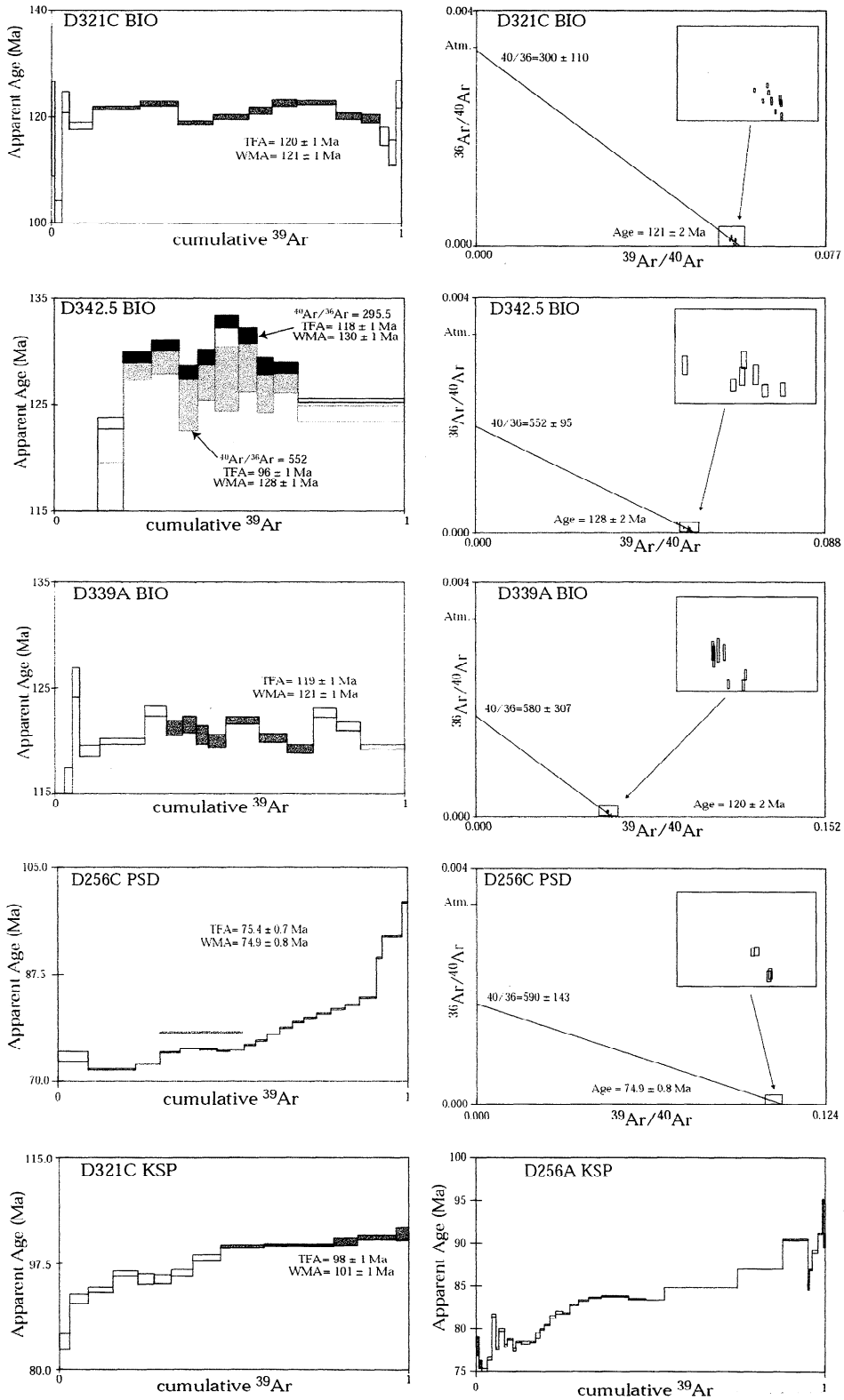

Figure 11. The ^{40}Ar/^{39}Ar age spectra and isotope correlation diagrams for samples that gave Cretaceous ages (D321C, D342.5, D339A, D256C, and D256A). Weighted mean ages were calculated using solid steps. Where two spectra are shown for a single sample, the older spectrum was calculated assuming a trapped ^{40}Ar/^{36}Ar ratio of 295.5, while the younger spectrum was calculated using the indicated ^{40}Ar/^{36}Ar ratio.

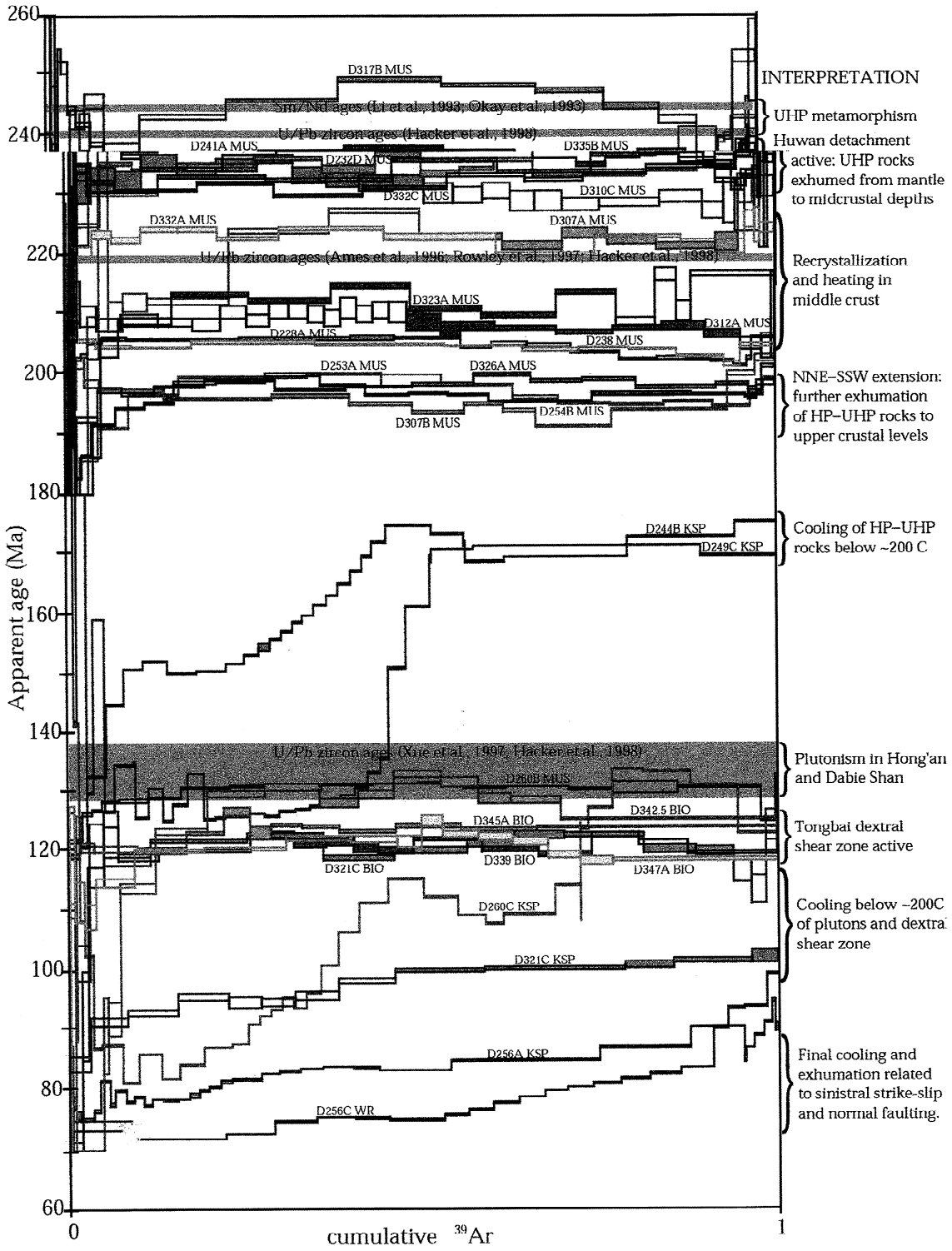

Figure 12. Summary spectra diagram of $^{40}Ar/^{39}Ar$ data (this study) with Sm/Nd and U/Pb ages (discussed in text) and tectonic interpretations. The $^{40}Ar/^{39}Ar$ data are those shown in Figures 6, 7, 8, and 9, and thus Figure 12 is meant to illustrate the clustering of ages with respect to Sm/Nd and U/Pb data.

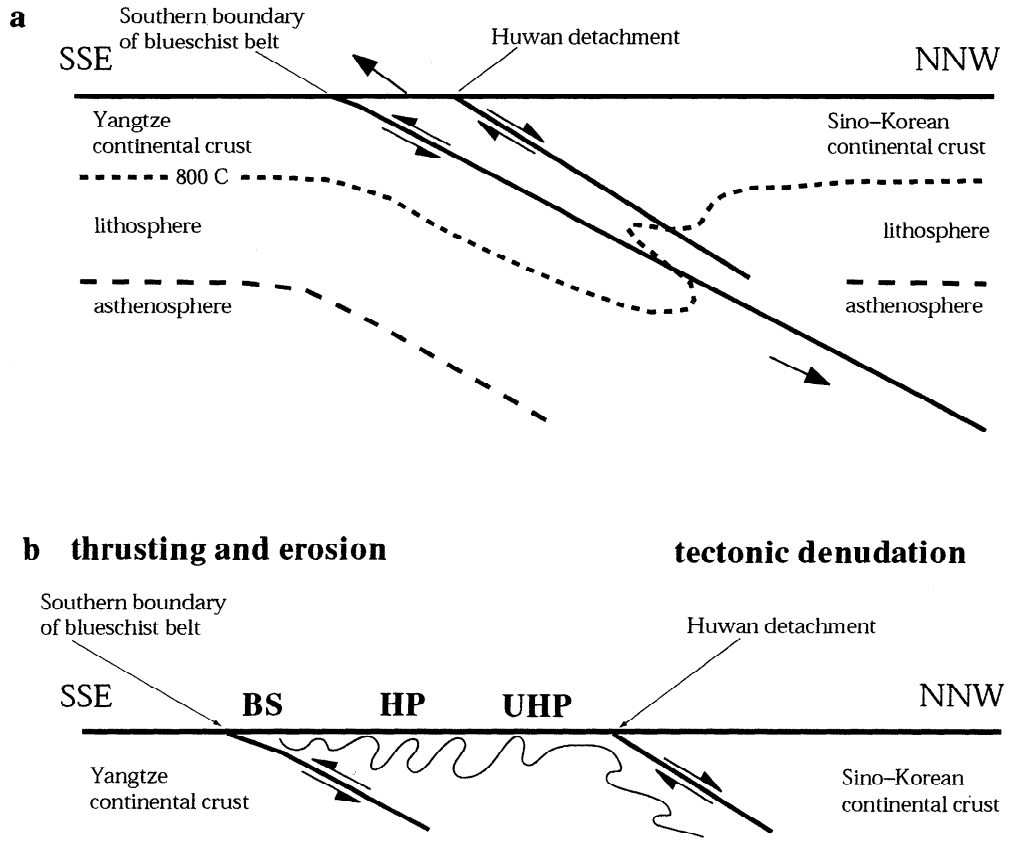

Figure 13. (a) Tectonic model for the exhumation of the ultrahigh-pressure rocks. Figure is modified from *Ernst and Peacock* [1996] and based on structural data presented here and by Webb et al. (submitted manuscript, 1999). Bowed isotherm illustrates how cooling is achieved along upper and lower boundaries of the exhuming slab as the HP–UHP rocks come into contact with cooler rocks. (b) Structures and relative locations of metamorphic units in the Hong'an Shan resulting from exhumation. Unroofing was facilitated by thrusting and erosion along the southern margin of the blueschist belt, and by tectonic denudation along the Huwan detachment. BS, blueschist unit; HP, high-pressure amphibolite and eclogite units; UHP, ultrahigh-pressure eclogite unit.

HP–UHP rocks were exhumed as a coherent slab, bounded above and below by north dipping normal and thrust faults, respectively (Webb et al., submitted manuscript, 1999; Hacker et al., manuscript in preparation, 1999). Models incorporating this scenario were previously published for the Dabie Shan [e.g., *Maruyama et al.*, 1994; *Ernst and Peacock*, 1996; *Liou et al.*, 1996] but lacked substantiating structural evidence. In these models, exhumation is driven by buoyancy forces due to density contrasts between the subducted crustal rocks and the overlying mantle lithosphere and/or continued contraction during collision. Corresponding physical models by *Chemenda et al.* [1995, 1996] suggest that underthrusting of continental lithosphere continues until a critical topographic height is reached. When erosional denudation removes this overburden, buoyancy forces drive the exhumation of subducted crust by formation of a normal fault above the exhuming slab and continued subduction below. Old, cold continental lithosphere enhances the depth from which these rocks can be exhumed [*Chemenda et al.*, 1996]. Such is the case with the collision between the Precambrian Yangtze and Sino–Korean cratons. This general model is attractive for explaining the preservation of UHP rocks in that cooling of the exhumed slab is achieved across both upper and lower surfaces [*Ernst and Peacock*, 1996] (Figure 13).

Extension associated with the Huwan detachement requires accommodation structures of the same age. Figure 14 illustrates how the Tan Lu might have initiated as a transfer fault during Middle to Late Triassic. If linked with thrust faults along the boundary between the blueschist unit and the fold-and-thrust belt, this model explains the termination of the fault at the southeastern tip of the Dabie Shan, and the resulting clockwise rotation is compatible with paleomagnetic data discussed earlier (i.e., clockwise rotation of the Yangtze craton as collision progressed from east to west).

Early Cretaceous extension and sinistral-oblique slip along the Xiaotian–Mozitan fault of the northern Dabie Shan resulted in the exhumation of rocks from depths of ~10–15 km [*Hacker et al.*, 1995]. This fault may be the eastward continuation of the Huwan detachment that was reactivated and overprinted during Cretaceous extension and plutonism. Consequently, HP–UHP rocks that resided at deeper crustal levels for a longer period of time are now exposed in the Dabie Shan, as opposed to the Hong'an and Tongbai Shan where Cretaceous deformation involved primarily strike-slip motion

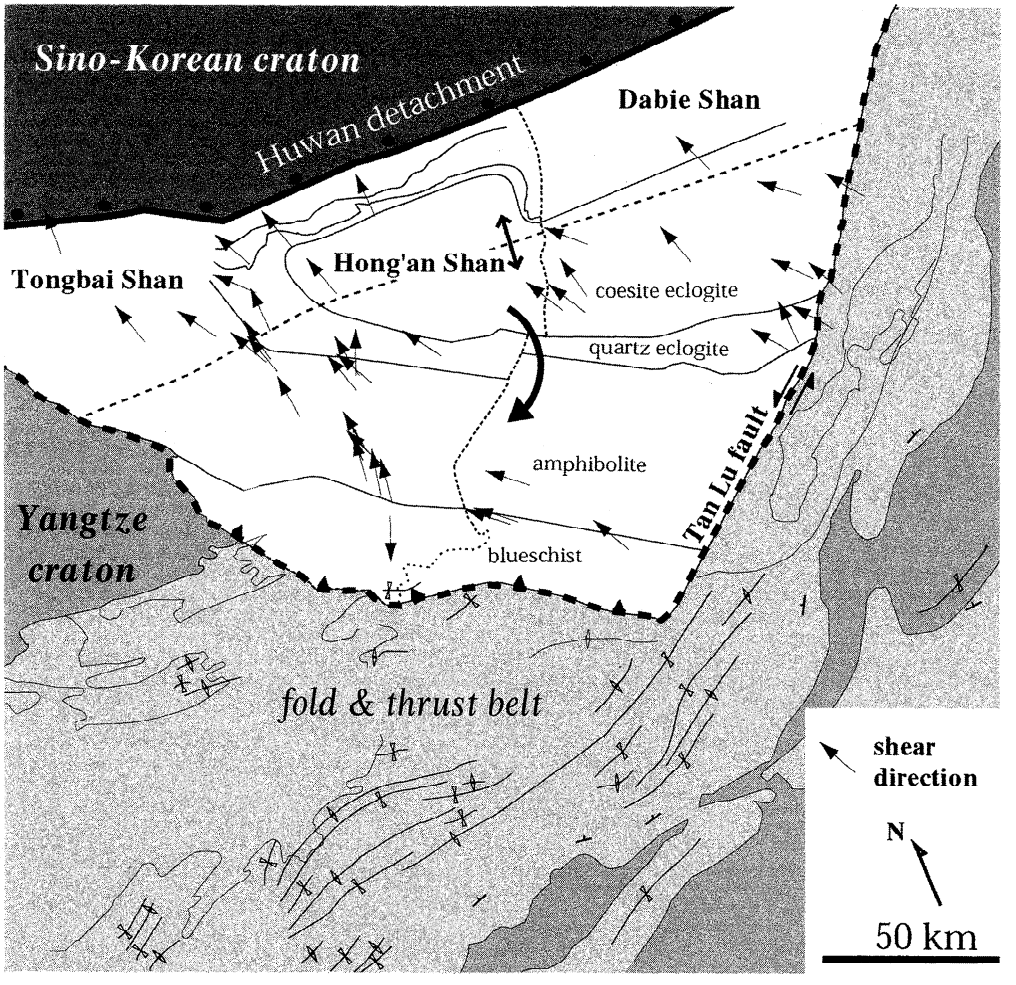

Figure 14. Pre-Cretaceous restoration of the Tongbai, Hong'an, and Dabie Shan modified after *Hacker et al.* [1998]. Arrow represents clockwise sense of rotation, the same as that documented by paleomagnetic data referenced in text. In this model, the Tan Lu originates in Middle to Late Triassic as a sinistral transfer fault that accommodates extension and continued contraction in the foreland as collision progressed westward.

and little or no exhumation. This is reflected by the larger population of Late Triassic to Early Jurassic $^{40}Ar/^{39}Ar$ ages reported from the Dabie Shan, as well as by the existence of voluminous retrograde amphibolite-facies tonalitic gneisses in the southern half of the range (e.g., the "amphibolite unit" of *Hacker et al.* [1995] and the "gray gneiss" of *Rowley et al.* [1997]). Thus the HP–UHP rocks of the Hong'an block do in fact best preserve the structure and cooling history associated with the bulk of exhumation from mantle depths.

Although *Hacker et al.* [1995] previously considered that the Dabie–Hong'an UHP rocks were exhumed through the mantle between ~227 and 200–180 Ma, ages presented here and by *Hacker et al.* [1998] suggest instead that exhumation from mantle depths of 120–150 km [e.g., *Hacker et al.*, 1997] to crustal depths occurred between ~240–245 Ma and ~235–230 Ma. The required exhumation rates are ~5–25 mm/yr.

5. Conclusions

North-northwest-down normal-sense shear along the Huwan detachment at the northern edge of the Hong'an block is constrained between 237 and 231 Ma by white mica cooling ages. Combined with U/Pb zircon and Sm/Nd ages of 245–240 Ma, this suggests that exhumation of UHP rocks through mantle depths occurred at rates of 5–25 mm/yr from ~245 to 230 Ma. The bulk of the mountain range is a warped extensional footwall, within which muscovites cooled by 205 Ma. Younger extension is recorded locally by white mica recrystallization at 198–194 Ma, after which the entire block had cooled to below 300°C.

The $^{40}Ar/^{39}Ar$ ages from the Tongbai shear zone indicate that dextral shear along the SW boundary of the orogen was contemporaneous with normal to sinistral-oblique slip along the Xiaotian–Mozitan fault of the northern Dabie Shan [*Hacker et al.*, 1995]. Coeval dextral and sinistral shear zones along the northern and southwestern margins of the Hong'an and Dabie Shan would have caused eastward lateral extrusion of these two blocks, perhaps driven by collision of the Lhasa block with Eurasia [*Allègre et al.*, 1984]. This deformation produced no significant exhumation of the UHP rocks.

Late Cretaceous–Eocene deformation included strike-slip faulting and extension. Structures related to this deformation

formed the major block-bounding faults for the Dabie Shan, Hong'an, and Tongbai regions.

Acknowledgments. This research was supported by U.S. National Science Foundation grant EAR-9417958, German National Science Foundation grants Ra442/4, 9, 14, Stanford–China Geosciences Industrial Affiliates Program, and a grant from the Stanford University McGee Fund. We would like to thank Andy Calvert and Phil Gans for running three of the samples at the University of California, Santa Barbara. Special thanks to Peng Lianhong for guidance in the field, to Mary Leech for field assistance in China, and to Dave Rowley, Frances Cole and Jaime Toro for their scientific insight. We also acknowledge Dave Scholl, An Yin and Gary Ernst for providing constructive reviews of the manuscript.

References

Allegrè, C. J., et al., Structure and evolution of the Himalaya–Tibet orogenic belt, *Nature*, *307*, 17-22, 1984.

Ames, L., G. Zhou, and B. Xiong, Geochronology and isotopic character of ultrahigh-pressure metamorphism with implications for collision of the Sino-Korean and Yangtze cratons, central China, *Tectonics*, *15*, 472-489, 1996.

Brugier, O., J. R. Lancelot, and J. Malavieille, U-Pb dating on single detrital zircon grains from the Triassic Songpan–Ganze flysch (Central China): Provenance and tectonic correlations, *Earth Planet. Sci. Lett.*, *152*, 217-231, 1997.

Chemenda, A. I., M. Mattauer, J. Malavieille, and A. N. Bokun, A mechanism for syn-collisional rock exhumation and associated normal faulting: Results from physical modelling, *Earth Planet. Sci. Lett.*, *132*, 225-232, 1995.

Chemenda, A. I., M. Mattauer, and A. N. Bokun, Continental subduction and a mechanism for exhumation of high-pressure metamorphic rocks: New modelling and field data from Oman, *Earth Planet. Sci. Lett.*, *143*, 173-182, 1996.

Chen, W., T. M. Harrison, M. T. Heizler, R. Liu, B. Ma, and J. Li, The cooling history of mélange zone in north Jiansu–south region: Evidence from multiple diffusion domain $^{40}Ar/^{39}Ar$ thermal geochronology, *Acta Pet. Sin.*, *8*, 1-17, 1992.

Eide, E. A., Petrology, geochronology, and structure of high-pressure metamorphic rocks in Hubei Province, east-central China, and their relationship to continental collision, Ph.D. thesis, 235 pp., Stanford Univ., Stanford, Calif., 1993.

Eide, E. A., M. O. McWilliams, and J. G. Liou, $^{40}Ar/^{39}Ar$ geochronologic constraints on the exhumation of high-pressure–ultrahigh-pressure metamorphic rocks in east-central China, *Geology*, *22*, 601-604, 1994.

Enkin, R. J., Z. Yang, Y. Chen, and V. Courtillot, Paleomagnetic constraints on the geodynamic history of the major blocks of China from the Permian to the Present, *J. Geophys. Res.*, *97*, 13,953-13,989, 1992.

Ernst, W. G., and S. M. Peacock, A thermotectonic model for preservation of ultrahigh-pressure phases in metamorphosed continental crust, in *Subduction: Top to Bottom*, *Geophys. Monogr. Ser.*, vol. 96, edited by G. E. Bebout et al., pp. 171-178, AGU, Washington D. C., 1996.

Hacker, B. R., and Q. Wang, Ar/Ar geochronology of ultrahigh-pressure metamorphic rocks in central China, *Tectonics*, *14*, 994-1006, 1995.

Hacker, B. R., L. Ratschbacher, L. E. Webb, and S. Dong, What brought them up?: Exhumation of the Dabie Shan ultrahigh-pressure rocks, *Geology*, *23*, 743-746, 1995.

Hacker, B. R., J. L. Mosenfelder, and E. Gnos, Rapid emplacement of the Oman ophiolite: Thermal and geochronologic constraints, *Tectonics*, *15*, 1230-1247, 1996a.

Hacker, B. R., X. Wang, E. A. Eide, and L. Ratschbacher, Qinling–Dabie ultrahigh-pressure collisional orogen, in *Tectonic Evolution of Asia*, edited by A. Yin and T. M. Harrison, pp. 345-370, Prentice-Hall, Englewood Cliffs, N. J., 1996b.

Hacker, B. R., L. Ratschbacher, L. E. Webb, T. Ireland, D. Walker, A. Calvert, and S. Dong, Exhumation of ultrahigh-pressure rocks, Dabie–Hong'an–Tongbai Shan, China, *Abstr. Programs, Geol. Soc. Am.*, *29*(6), 469, 1997.

Hacker, B. R., L. Ratschbacher, L. E. Webb, T. Ireland, D. Walker, and S. Dong, U/Pb Zircon ages constrain the architecture of the ultrahigh-pressure Qinling-Dabie orogen, China, *Earth Planet. Sci. Lett.*, *161*, 215-230, 1998.

Li, S., and T. Wang, *Geochemistry of Granitoids in the Tongbaishan-Dabieshan, Central China*, China Univ. of Geosci. Press, Wuhan, 1991.

Li, S., S. R. Hart, S. G. Zheng, D. L. Liou, and A. Guo, Sm-Nd isotopic evidence for timing of the collision between the north and south China cratons: The Sm-Nd isotopic evidence, *Sci. China Ser. B*, *32*, 1391-1400, 1989a.

Li, S., S. R. Hart, S. G. Zheng, D. L. Liou, G. W. Zhang, and A. Guo, Timing of collision between the north and south China blocks: The Sm-Nd evidence, *Sci. China ser. B*, *32*, 1393-1400, 1989b.

Li, S., et al., Collision of the North China and Yangtze and formation of coesite-bearing eclogites: Timing and processes, *Chem. Geol.*, *109*, 89-111, 1993.

Lin, J. L., M. Fuller, and W. Zhang, Preliminary Phanerozoic polar wander paths for the North and South China blocks, *Nature*, *313*, 444-449, 1985.

Liou, J. G., R. Y. Zhang, X. Wang, E. A. Eide, W. G. Ernst, and S. Maruyama, Metamorphism and tectonics of high-pressure and ultra-high-pressure belt in the Dabie–Sulu region, China, in *Tectonic Evolution of Asia*, edited by A. Yin and T. M. Harrison, pp. 300-344, Prentice-Hall, Englewood Cliffs, N. J., 1996.

Maruyama, S., J. G. Liou, and R. Zhang, Tectonic evolution of the ultrahigh-pressure (UHP) and high-pressure (HP) metamorphic belts from central China, *Isl. Arc*, *4*, 112-121, 1994.

Mattauer, M. P., H. Matte, Z. Maluski, X. Xu, Y. Lu., and Y. Tang, Tectonics of the Qinling Belts, build-up and evolution of eastern Asia, *Nature*, *327*, 496-500, 1985.

Okay, A. I., and A. M. C. Sengör, Evidence for intracontinental thrust-related exhumation of the ultra-high-pressure rocks in China, Geology, *20*, 411-414, 1992.

Okay, A. I., A. M. C. Sengör, and M. Satir, Tectonics of an ultrahigh-pressure metamorphic terrane: Dabie Shan, China, *Tectonics*, *12*, 1320-1334, 1993.

Opdyke, N. D., K. Huang, G. Xu, W. Y. Zhang, and D. V. Kent, Paleomagnetic results from the Triassic of the Yangtze Platform, *J. Geophys. Res.*, *91*, 9553-9568, 1986.

Peltzer, G., and P. Tapponnier, Formation and evolution of strike-slip faults, rifts, and basins durign the India–Asia collision: An experimental approach, *J. Geophys. Res.*, *93*, 15,085-15,117, 1988.

Peltzer, G., P. Tapponnier, Z. Zhang, and Z. Q. Xu, Neogene and Quaternary faulting in and along the Qinling Shan, *Nature*, *317*, 500-505, 1985.

Regional Geological Survey Anhui (RGS Anhui), *Regional Geology of the Anhui Province*: Geological, Beijing, 1987.

Regional Geological Survey Henan (RGS Henan), *Regional Geology of the Henan Province*: Geological, Beijing, 1989.

Regional Geological Survey Hubei (RGS Hubei), *Regional Geology of the Hubei Province*: Geological, Beijing, 1990.

Rowley, D. B., and F. Xue, Modeling the exhumation of ultra-high pressure metamorphic assemblages: Observations from the Dabie/Tongbai region, China, *Abstr. Programs, Geol. Soc. Am.*, *28*(7), 249, 1996.

Rowley, D. B., F. Xue, R. D. Tucker, Z. X. Peng, J. Baker, and A. Davis, Ages of ultrahigh pressure metamorphism and protolith orthogneisses from eastern Dabie Shan: U/Pb zircon geochronology, *Earth Planet. Sci. Lett.*, *151*, 191-203, 1997.

Wang, X., and J. G. Liou, Regional ultrahigh-pressure coesite-bearing eclogitic terrane in central China: Evidence from country rocks, gneiss, marble and metapelite, *Geology*, *19*, 933-936, 1991.

Webb, L. E., B. R. Hacker, L. Ratschbacher, and S. Dong, Structures and kinematics of exhumation: Ultrahigh-pressure rocks in the Hong'an Block of Qinling-Dabie Orogen, China, *Abstr. Programs, Geol. Soc. Am.*, *28*(7), 69, 1996.

Xue, F., D. B. Rowley, R. D. Tucker, and Z. X. Peng, U-Pb zircon ages of granitoid rocks in the North Dabie Complex, eastern Dabie Shan, China, *J. Geol.*, *105*, 744-753, 1997.

Yin, A., and S. Nie, An indentation model for the North and South China collision and the development of the Tanlu and Honam fault systems, eastern Asia, *Tectonics*, *12*, 801-813, 1993.

Zhang, R. Y., J. G. Liou, and B. L. Cong, Discovery of coesite in eclogites from Henan Province, central China and its tectonic implications, *Abstr. Programs Geol. Soc. Am.*, *25*(5), 169, 1993.

Zhou, D., and S. A. Graham, Songpan-Ganzi complex of the west Qinling Shan as a Triassic remnant-ocean basin, in *Tectonic Evolution of Asia*, edited by A. Yin and T. M. Harrison, Prentice-Hall, Englewood Cliffs, N. J., 1996.

S. Dong, Institute of Geomechanics, Chinese Academy of Geological Sciences, No. II Ming Zhu Xueyang South Rd., 100081 Beijing, China

B. R. Hacker, Department of Geological Sciences, University of California at Santa Barbara, Santa Barbara, CA 93106-9360. (hacker@magic.geol.ucsb.edu)

M.O. McWilliams, Department of Geological and Environmental Sciences, Stanford University, Stanford, CA 94305-2115. (mac@pangea.stanford.edu)

L. Ratschbacher, Institute for Geology, Universitaet Wuerzburg, Pleicherwall 1, Wuerzburg, D 97070 Germany. (lothar@geologie.uni-wuerzburg.de)

L. F. Webb, Section des Sciences de la Terre, University of Geneva, 13 Rue des Maraichers, 1211 Geneva 4, Switzerland. (Laura.Webb@terre.unige.ch)

(Received November 2, 1998;
revised March 11, 1999;
accepted March 29, 1999)